Angular Dependence in Static and Dynamic Light Scattering from Randomly Branched Systems

V. Trappe,[†] J. Bauer,[‡] M. Weissmüller,[†,§] and W. Burchard*[,†]

Institute of Macromolecular Chemistry, University of Freiburg, D-79104 Freiburg, Germany, and Fraunhofer-Institute of Applied Materials Research, D-14513 Teltow, Germany

Received November 26, 1996; Revised Manuscript Received February 7, 1997[⊗]

ABSTRACT: The static and dynamic properties of three randomly branched systems under good solvent conditions have been investigated by light scattering. Despite large differences in the topology and chemical structure of these systems one common scaled particle scattering function ($P(qR_g)$) is obtained for the probed q range. In dynamic light scattering, however, the topological differences have a significant effect. At high q values the first cumulant $\Gamma(q)$ exhibits a $q^{2.8}$ dependence for the systems with small repeating units and a q^3 dependence for the system with the largest repeating unit. These dependencies indicate internal motions with strong hydrodynamic interactions (Zimm-like behavior). The *absolute* values of the reduced cumulant $\Gamma^*(q) \equiv \Gamma(q)\eta_o/(q^3kT)$ at high q values proved to be a sensitive measure of the internal mobility, and information on the internal structure of polymers can be deduced from these values. By comparison of the $\Gamma^*(q)$ values from the branched systems with those from linear systems under Θ and good solvent conditions the nature of the local dynamics in the various systems is classified: for the system with the largest repeating unit the local dynamics of *linear* sections of the clusters are registered, whereas for the systems with smaller repeating unit, i.e. higher branching density, the local dynamics of *branched* sections are probed.

Introduction

In this paper we present data on the angular dependencies in static and dynamic light scattering from three randomly branched systems which differ considerably in their chemical and topological structure. In particular the large differences in size of their basic units (referred hereafter as unimers) are to be pointed out, which range from $M_o = 417$ g/mol to about $M_o = 65\,000$ g/mol. When probing the different systems at small length scales, we expect the size of the unimer to have a determining effect, and the differences should become apparent.

The relevant structural quantities can be investigated by light scattering (LS) when the probed clusters are sufficiently large such that the structure sensitive regime of $qR_g > 1$ is covered by the limited q range of light scattering. Here, R_g is the radius of gyration and $q = (4\pi n_o/\lambda_o)\sin(\theta/2)$, the magnitude of the scattering vector with λ_o the wavelength of the light, θ the scattering angle and n_o the refractive index of the solvent used. The condition $qR_g > 1$ is easily fulfilled with randomly branched polymers, since in the course of the branching process very large clusters are formed.[1] Simultaneously the size distribution broadens, and the resulting extremely large polydispersities of the samples have to be taken into account when analyzing the scattering behavior properly.

In static light scattering power law behavior of the scattered light as a function of q is often observed when $qR_g \gg 1$, and the resulting exponent should give the fractal dimension d_{fr} of the individual clusters. For randomly branched systems, however, the large polydispersity has a significant effect on the scattering behavior, resulting in an ensemble fractal dimension $d_{fr,e}$, which is related to d_{fr} by $d_{fr,e} = d_{fr}(3 - \tau)$ where τ is the exponent describing the power law decay in the number distribution of the randomly branched clusters.[2] Much work has been done already on the static properties[3] of branched systems, but far less attention has been paid to the dynamics. It is known that the dynamics of linear, flexible chains in dilute solution are governed by strong hydrodynamic interactions, and a qualitatively satisfying agreement of the experimental findings with theoretical predictions has been obtained.[4] For randomly branched clusters, however, little is known[5] about the internal segmental motion and whether branching has an influence on the mobility and hydrodynamic interaction. Also, while the effect of polydispersity is well understood in static LS, the corresponding influence in dynamic LS has not yet been clarified. For instance, there may be a q-regime where the smaller clusters of the ensemble are still in a translational regime while the internal motions of the larger ones are probed. The relevant function that can be measured by dynamic LS is the field time correlation function (TCF) which, similar to the particle scattering factor measured by static LS, shows an angular dependence that in the present paper will be analyzed in detail.

The Systems

(1) Cross-linked polycyanurates (c-PCyan) were synthesized by poly(cyclotrimerization) of dicyanates of bisphenol-A. The reactions were conducted in the melt at 190 °C, well above the glass transition temperature, and different extents of branching were obtained by quenching the reaction medium after different times of reaction before gelation. Further details are given in ref 6.

(2) Cross-linked polyester chains (c-PEst-chain) were obtained by copolymerization in bulk of phenyl glycidyl ether (PGE), bisphenol-A-diglycidyl ether (BADGE) and phthalic acid anhydride (PA). 1-methylimidazol (1-MI) was used as initiator. The anhydride curing of epoxies initiated by tertiary amines was shown to follow a living chain mechanism,[7] such that by curing monoepoxies, e.g. PGE, fairly monodisperse chains are

[†] University of Freiburg.
[‡] Fraunhofer-Institute of Applied Materials Research.
[§] Present address: CRT Analytisches Laboratorium, Hoechst AG, D-65926 Frankfurt am Main, Germany.
[⊗] Abstract published in *Advance ACS Abstracts,* April 1, 1997.

S0024-9297(96)01728-7 CCC: $14.00

Scheme 1

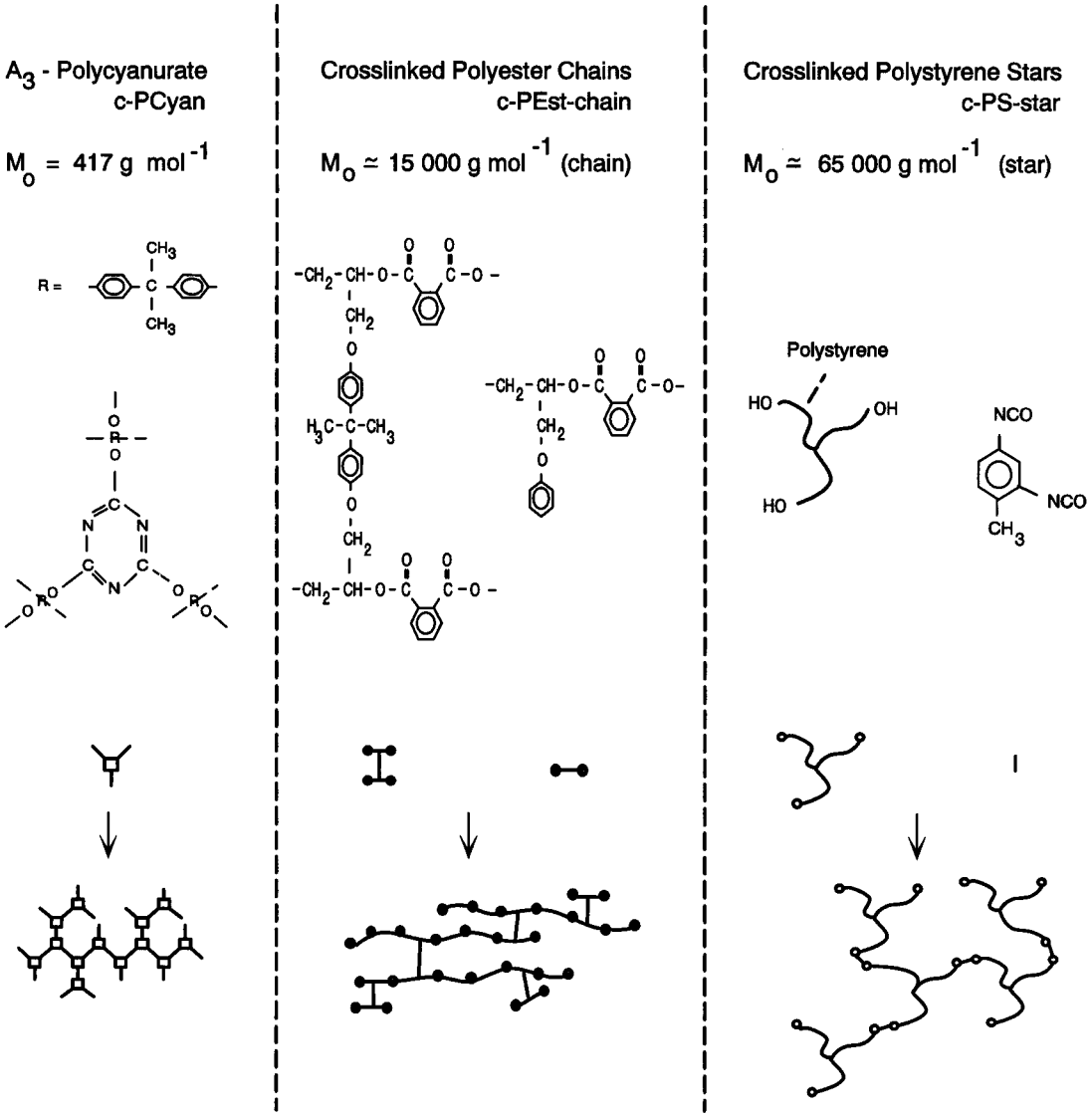

obtained.[8] Branched materials were synthesized by curing defined mixtures of diepoxy, BADGE, and monoepoxy, PGE, in which BADGE acts as crosslinker. The reaction was conducted to complete epoxy consumption. Samples with different branching densities were obtained by varying the amount of crosslinker per chain (X = [BADGE]/[1-MI]), while the length of the primary chain, defined by the ratio of the epoxy to initiator concentration, was kept constant ([Epoxy]/[1-MI] = 50; $M_o \cong 15\,000$ g mol^{-1}). The primary chain establishes here the unimer.

(3) Uniform 3-arm polystyrene stars ($M_o \cong 65\,000$ g mol^{-1}) with terminal OH groups were crosslinked by reaction with toluene 2,4-diisocyanate in 20% (w/v) toluene solutions (c-PS-star system). Similar to the polyester system, variation in branching density was achieved by varying the ratio of the number of isocyanate endgroups to the number of hydroxy groups (r = [NCO]/[OH]) where the reactions were led to complete NCO-consumption. Details of the rather complex preparation of the star molecules and the crosslinking will be given in a separate paper.

In Scheme 1 the chemical and spatial structures of the three systems are shown. Both the c-PCyan system and the c-PS-star system represent systems of randomly branched trifunctional units, though their units differ strongly in size and flexibility. In contrast the c-PEst-chain system is an ensemble of randomly crosslinked, fairly monodisperse chains. As already mentioned the three systems differ especially in the size of their basic units, their unimers. The unimer size increases in order: c-PCyan (M_o = 417 g/mol) < c-PEst-chain ($M_o \cong$ 15 000 g/mol) < c-PS-star ($M_o \cong$ 65 000 g/mol).

Experimental Section

Series of five to six concentrations (0.1 g/L < concentration < 10 g/L) were prepared from each of the various samples of the three systems described above. In all cases tetrahydrofuran (THF) was used as solvent, which for these systems has similar good solvent qualities. All solutions were filtered five to six times through Millipore Teflon filters. Depending on the molar mass of the samples different pore sizes of the filters were chosen (0.2, 0.5, 5 μm). The used glassware and the cylindrical light scattering cells (diameter 0.8 cm) were rinsed with freshly distilled acetone in a special rinsing apparatus in order to remove adhered dust particles. All cleaning procedures were carried out in a laminar flow box.

Static light scattering measurements were performed with two modified and fully computerized SOFICA photogoniometers (G. Baur, SLS-Systemtechnik, Hausen), where a 2 mW HeNe laser (λ_o = 632.8 nm, Uniphase) and a 5 mW Ar-ion laser (λ_o = 488 nm, Uniphase) were used as light sources. In addition static light scattering measurements were per-

formed simultaneously with *dynamic light scattering* experiments using two ALV photogoniometers (ALV GmbH, Langen, Hessen), where a 3 W Ar-ion laser (λ_o = 457.9 nm and λ_o = 488 nm, Spectra-Physics 2000) and 750 mW Kr-ion laser (λ_o = 647.1 nm, Spectra-Physics 2020) were used as light sources. The used equipment and the calibration-proceedure are described in ref 9. Most of the time correlation functions (TCF) were determined with an ALV 3000 autocorrelator; the ALV-5000 became available to us only for the experiments on the c-PS-star system. The scattering measurements were made in an angular range of 20−150° in steps of 5° (q-range: 4.7×10^4 to 3.7×10^5 cm^{-1}).

The refractive index increments were measured with a Brice Phoenix differential refractometer for different wavelengths and the following results were obtained: c-PCyan, dn/dc = 0.185 cm^3/g (λ_o = 647.1 nm); c-PEst-chain, measured for 6 different wavelengths, dn/dc = 0.137 + 5.84 × 10^3 λ_o^{-2} (λ_o in nm and dn/dc in cm^3/g); c-PS-star, dn/dc = 0.185 cm^3/g (λ_o = 633 nm), dn/dc = 0.195 cm^3/g (λ_o = 488 nm).

The measurements were carried out at 20 °C for the c-PCyan and the c-PS-star systems and at 25 °C for the c-PEst-chain system.

For the calculation of the hydrodynamic radius, according to the Stokes−Einstein relation $R_h = kT/(6\pi\eta_o D_z)$, and the calculation of $\Gamma^*(q) = \Gamma(q)\eta_o/(kTq^3)$ the following solvent viscosities (η_o) were used: THF/20 °C η_o = 0.47 cP; THF/25 °C η_o = 0.46 cP.

The first cumulant $\Gamma(q)$ was determined by a three-cumulant fit of the field time correlation function $g_1(q,t)$. In particular for the correlation functions at high qR_g, it was necessary to restrict the fit to values of $g_1(q,t) > 0.65$. According to our experience the determination of $\Gamma(q)$ on TCFs obtained in *single* τ mode is more accurate than on TCFs obtained in *multi* τ mode, since for the initial part of the correlation function more data are produced in the single τ mode.

All q-dependent data (Kc/R_θ, $D_{app}(q) = \Gamma(q)/q^2$) presented here result from linear extrapolation to zero concentration of the corresponding data measured for the dilute solutions of various concentrations. For smaller samples R_g, M_w, and D_z were determined by linear extrapolation to $q = 0$ in Zimm diagrams. For the large samples different procedures were used: higher order fits in Zimm diagrams, Berry diagrams, and Guinier diagrams; fitting according to eqs 2 and 5 (see Results and Discussion), using an ensemble fractal dimension $d_{fr,e}$ as obtained by linear regression of log(R_θ/Kc) vs log(q) in the high q regime.

Results and Discussion

Before comparing the static and dynamic behavior of the three different systems described above, some general features of the q dependencies, obtained for samples at different extent of branching, shall be demonstrated. As a representative example the data obtained for five samples of the PEst-chain system are displayed in detail in the following Figures 1 and 2. The molecular characteristics of these samples are listed in Table 1.

Figure 1A shows the double logarithmic plots of R_θ/Kc and $D_{app}(q)$ vs q. The static and dynamic properties exhibit corresponding behavior. With increasing R_g, more and more of a limiting power-law behavior becomes noticeable in the q-regime of light scattering. The data of Figure 1A can also be plotted in the normalized forms $P(q) = R_\theta/R_{\theta=0}$ and $D_{app}(q)/D_z$ as shown in Figure 1B, where qR_g is used as dimensionless length scale. For both static structure and dynamics, the curves collapse to one common master curve. This almost perfect collapse is a result of the self-similar character of randomly branched clusters.[11] It is worth emphasizing that with progressing branching reaction the size distribution broadens; the higher moments of the distribution increase, whereas the first moment remains approximately constant. The polydispersity ratio M_w/M_n of the investigated samples increases with increasing weight average molar mass M_w. In spite of this variation in the width of the distribution a common behavior is observed due to the fact that randomly branched clusters are fractal in a twofold manner: First, each single cluster is a fractal of dimension d_{fr}, and second, the cluster ensembles at different extents of branching are self-similar to each other. Both self-similarities eventually result in the ensemble fractal dimension $d_{fr,e}$ of the non fractionated samples.

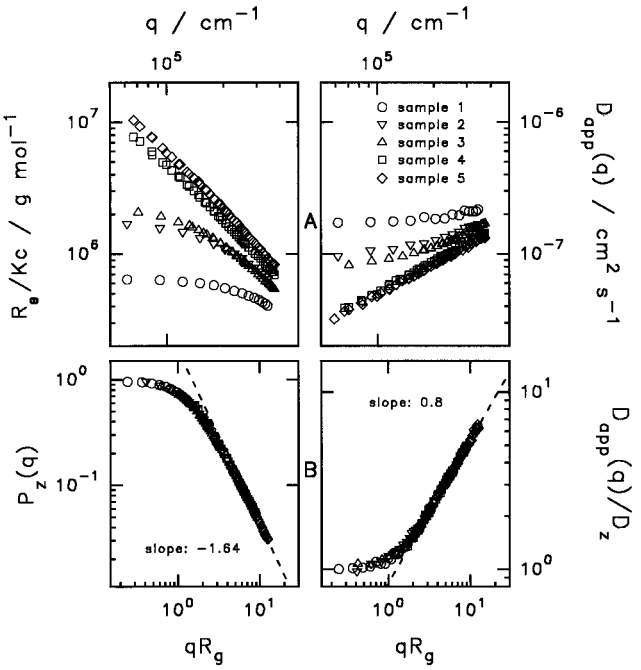

Figure 1. (A) R_θ/Kc and $D_{app}(q) = \Gamma(q)/q^2$ as a function of q for five c-PEst-chain samples. (B) Corresponding normalized plots: $P_z(q) = R_\theta/R_{\theta=0}$ and $D_{app}(q)/D_z$ vs qR_g. The radius of gyration R_g increases with the sample number (further characteristics in Table 1).

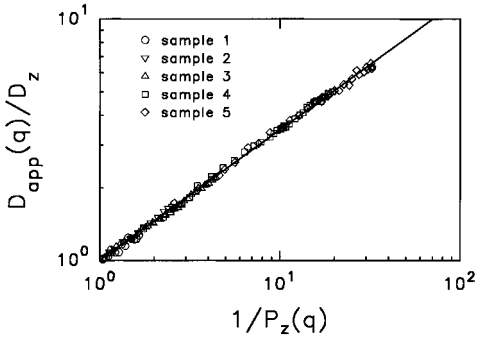

Figure 2. Double logarithmic plot of $D_{app}(q)/D_z$ vs $1/P_z(q)$ for the c-PEst-chain system.

Table 1. Molecular Characteristics of Five c-PEst-Chain Samples in THF at 25 °C

sample	X	M_w/M_n	M_w	R_g/nm	R_h/nm
1	0.801	20	6.69×10^5	39.8	27.6
2	0.810	50	1.77×10^6	67.1	48.4
3	0.842	67	2.40×10^6	89.3	61.1
4	0.867	370	1.36×10^7	245	164
5	0.887		2.70×10^7	341	224

[a] X is the parameter defining the number of branching-points per chain. The gel-point was determined[9] to be $X_c = 0.886 \pm 0.006$. Sample 5 was therefore synthesized in the vicinity of the gel-point.

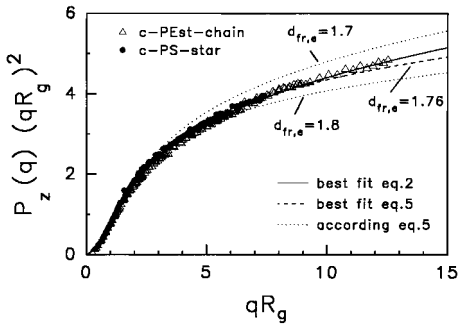

Figure 3. Kratky plot of the static LS data obtained for the c-PEst-chain system and c-PS-star system.

Inspection of Figure 1B reveals that the angular dependence of the static and dynamic LS data exhibit close similarities. In particular the transition range from initial to asymptotic behavior appears to be identical. In fact, a nearly straight line is obtained when plotting $D_{app}(q)/D_z$ vs $P(q)^{-1}$ in a double logarithmic scale (Figure 2). This allows us to express the dynamic LS data in terms of the static measurements:

$$D_{app}(q) = D_z P(q)^{-m} \tag{1}$$

An exponent $m = 0.54 \pm 0.02$ is found for the data of the c-PEst-chain system.

For static light scattering it is known[3] that the structure and polydispersity of the randomly branched clusters determine the q-dependence. The scaling behavior observed in Figure 2 seems to imply that, at least for the length scales probed by light scattering, these structural and polydispersity characteristics have a similar influence on the q dependence in dynamic LS.

We now turn to the detailed discussion of the static and dynamic behavior of the three systems c-PCyan, c-PEst-chain, and c-PS-star.

Static Light Scattering. In Figure 3 the normalized static LS data of the c-PEst-chain and the c-PS-star systems are presented in a Kratky plot, in which by multiplication of the form factor $P(q)$ with $(qR_g)^2$ the asymptotic part is emphasized, such that small differences between the various data sets can be easily detected. Clearly, there are no differences within the limit of experimental error. The data of the PCyan system obtained by Bauer et al.[12] exhibit exactly the same behavior, and are not shown in Figure 3 for the sake of clarity.

The fact that the three systems exhibit identical scaling behavior (at least for the investigated qR_g regime up to qR_g = ca. 10) is worth emphasizing, because the unimers of these systems are very dissimilar to each other. In the c-PCyan system the unimer is a low molecular weight monomer, it is small, rigid and disk-like in shape. In the c-PEst-chain system the basic unit is a flexible, narrowly distributed chain that is more than 20 times larger than the c-PCyan unimer, and in the c-PS-star system the star unimer has long, flexible arms and is more than 80 times larger than the c-PCyan unimer. The resulting clusters differ in the spacing of their branching points and in the functionality of the branching points (three in c-PCyan and c-PS-star; four in c-PEst-chain). The static scattering is apparently not affected by these topological details and seems to be purely dominated by the simple concept of connectivity in the ensemble of random branched clusters, which is for the different systems presumably the same.

To describe the experimental master curve the following empirical approximation[13] can be used

$$P(q) = (1 + a(qR_g)^2)^{-d_{fr,e}/2} \tag{2}$$

with

$$a = \frac{2}{3d_{fr,e}}$$

which fulfills the required conditions in the two limiting regimes:

$$qR_g \ll 1: \quad P(q) = \left(1 + \frac{1}{3}(qR_g)^2\right)^{-1} \tag{3}$$

$$qR_g \ll 1: \quad P(q) \sim (qR_g)^{-d_{fr,e}} \tag{4}$$

The bold line in Figure 3 represents the best fit for the c-PEst-system with $a = 0.44 \pm 0.01$ and $d_{fr,e} = 1.64 \pm 0.02$, which agrees with the value of $d_{fr,e} = 1.64 \pm 0.04$ obtained by linear regression in the double logarithmic plot of $P(q)$ vs qR_g shown in Figure 1B (light scattering regime, qR_g up to 12). To fulfill eq 3 properly parameter a should be set to $a = {}^2/_3 d_{fr}$. We nevertheless decided to fit our data with two free parameters to get a more accurate description of the experimental behavior. The deviation from the expected value of $a = 0.41 \pm 0.01$ is small and can be regarded as insignificant.

Bauer et al.[12] studied the static properties of the c-PCyan-system over a large range of q by combining light scattering and small-angle X-ray scattering (SAXS). They showed first that the data could be well fitted by a function derived by Freltoft et al.[14] for fractal aggregates

$$P(q) = \frac{\sin[(d_{fr,e} - 1)\arctan(q\xi)]}{(d_{fr,e} - 1)q\xi(1 + q^2\xi^2)^{(d_{fr,e}-1)/2}} \tag{5}$$

where

$$\xi^2 = \frac{2}{d_{fr,e}(d_{fr,e} + 1)} R_g^2 \tag{6}$$

For the c-PCyan and the c-PEst-chain systems a best fit is now obtained with $d_{fr,e} = 1.76 \pm 0.01$, which for the c-PCyan system agrees with the fractal dimension obtained by a linear regression according to eq 4 in the SAXS regime[12] (qR_g up to 10^3). The fractal dimension can also be determined from the M_w dependence of R_g according to

$$M_w \sim R_g^{d_{fr,e}} \tag{7}$$

For the c-PCyan system[12] $d_{fr,e} = 1.74 \pm 0.02$ and c-PEst-chain system[10] $d_{fr,e} = 1.78 \pm 0.08$ were obtained in good agreement with the findings according to eq 5. From these results it becomes obvious that the ensemble fractal dimension is underestimated when determined by linear extrapolation in the high q regime of light scattering according to eq 4 or by fitting the data according to eq 2. A similar underestimation of $d_{fr,e}$ was reported by Martin et al.[3e] for a silica gel system.

Examining eq 5 in the asymptotic region of $q\xi \gg 1$ the reason for these underestimates becomes apparent. In this limit $\arctan(q\xi) \rightarrow \pi/2$ and eq 5 becomes

$$P(q) \sim (q\xi)^{-d_{fr,e}} \tag{8}$$

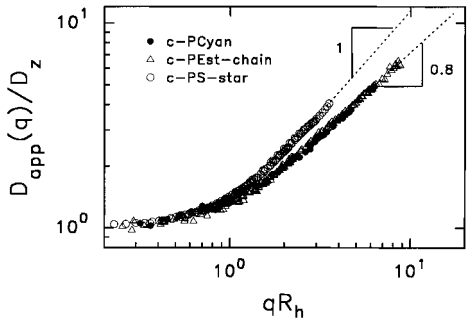

Figure 4. Variation of $D_{app}(q)/D_z$ as a function of qR_h for the three investigated systems: c-PCyan, c-PEst-chain and c-PS-star.

With eq 6 and $d_{fr,e} \cong 1.76$ one gets

$$q\xi = qR_g/1.56 \tag{9}$$

which means that $qR_g > 15$ has to be reached before $q\xi \gg 1$ is fulfilled, a regime which is normally not accessible by light scattering even if very large clusters ($R_g \cong 400$ nm) are investigated.

However, as seen from the curves (dotted lines) in Figure 3, the absolute values of the form factor, emphasized by the Kratky normalization, vary sufficiently with $d_{fr,e}$ at $qR_g > 8$, that conclusions on the internal structure can be drawn even if the asymptotic regime is not yet reached.

Using the percolation prediction[2]

$$d_{fr,e} = d_{fr}(3 - \tau) \tag{10}$$

and

$$\tau = 2.2$$

one finally obtains with $d_{fr,e} = 1.76 \pm 0.04$ the fractal dimension for the individual clusters $d_{fr} = 2.20 \pm 0.05$, which indicates fairly swollen clusters.

Dynamic Light Scattering: The First Cumulant. In theories[15] on dynamic LS from flexible linear chains ν-dependent master curves are predicted when $D_{app}(q)/D_z$ is expressed in terms of qR_g. The parameter ν is defined through the equation $R_g \sim M_w^{\nu}$ and describes the solvent quality ($\nu = 1/2$ for Θ conditions and $\nu = 3/5$ for good solvent conditions). The apparent diffusion coefficient is defined as $D_{app}(q) = \Gamma(q)/q^2$. An asymptotic power law behavior $D_{app}(q) \sim q^n$ [$\Gamma(q) \sim q^{n+2}$] has been predicted[16] with an exponent of $n = 1$ for chains with strong hydrodynamic interactions (Zimm[17] limit) and $n = 2$ for fully screened hydrodynamic interactions (Rouse[18] limit).

Figure 4 demonstrates that scaling is also obtained for the branched systems. Here qR_h is chosen as a dimensionless length scale. The ratio $\rho = R_g/R_h$ is for a given system independent of the molar mass indicating that the crossover region is already passed. However, ρ varies from one system to another. Thus, the curves for the different systems are shifted by different factors when plotted vs a qR_g scale instead of the qR_h scale used here. Obviously the diffusion coefficients of the branched c-PCyan and c-PEst-chain systems do not increase linearly with q as predicted and experimentally found for monodisperse, linear systems, but follow in the high qR_h regime a power-law of $D_{app}(q) \sim q^{0.8\pm0.05}$. The same behavior was found for the silica gel system investigated by Martin et al.[5c] In contrast a linear q dependence of $D_{app}(q) \sim q^{1\pm0.05}$ is found for the c-PS-star system and was also reported for the radical copolymer of styrene and divinylbenzene investigated by Delsanti et al.[5d] In terms of the first cumulant the asymptotic power law varies in these examples between $\Gamma(q) \sim q^{2.8}$ and $\Gamma(q) \sim q^3$.

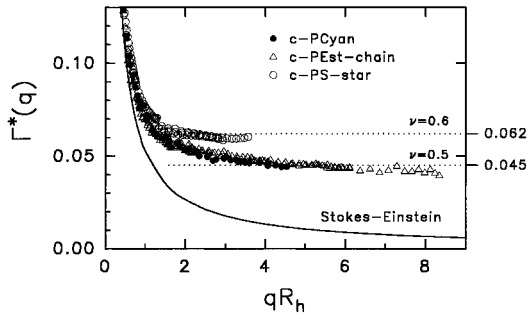

Figure 5. Variation of $\Gamma^*(q)$ as function of qR_h for the three investigated systems: c-PCyan, c-PEst-chain, and c-PS-star. The bold line represents the translational behavior $\Gamma^*(q) \sim q^{-1}$. The dotted line corresponds to the plateau values found experimentally for linear systems at Θ solvent conditions ($\nu = 1/2$; $\Gamma^*(\infty) \cong 0.045$)[4c,4d] and good solvent conditions ($\nu = 3/5$; $\Gamma^*(\infty) \cong 0.062$)[4f,4h].

When plotting the data as $\Gamma^*(q)$ vs qR_h (Figure 5) the differences between the behavior of the various branched systems are even more clearly demonstrated. $\Gamma^*(q)$ is defined as

$$\Gamma^*(q) \equiv \left(\frac{\Gamma(q)}{q^3}\right)\left(\frac{\eta_o}{kT}\right) \tag{11}$$

It is a dimensionless quantity, but includes *no* polymer specific normalization. When, as expected for linear chains in the Zimm limit, a q^3 dependence of the first cumulant is reached $\Gamma^*(q)$ reaches a constant value $\Gamma^*(\infty)$, which is predicted[15] to decrease with ν.

For the systems with comparatively small basic units, c-PCyan and c-PEst-chain, the Γ^* values decrease continuously even below the values found experimentally for linear systems under Θ conditions ($\nu = 1/2 \Rightarrow d_{fr} = 2$, $\Gamma^*(\infty) \cong 0.045$; see ref 4c, 4g). For the c-PS-star system, on the other hand, an asymptotic $\Gamma^*(\infty)$ value is reached, which agrees well with that found for linear chains in good solvents ($\nu = 3/5 \Rightarrow D_{fr} = 1.67$, $\Gamma^*(\infty) \cong 0.062$; see ref 4f,h) and in particular coincides with the asymptote of the corresponding linear system, polystyrene chains in THF.[4h]

Tetrahydrofuran (THF), the solvent used for all three systems under discussion, has similar good solvent properties for these systems. It is therefore unlikely that the variance in dynamical behavior is based on differences in excluded volume. Rather the difference in size of the basic unit appears to be the reason for the disparity. Two effects have to be taken into consideration. (i) With increasing size of the basic unit the scale on which *linear* segments in the clusters are probed increases. (ii) At a given molar mass the degree of unimer polymerization decreases as the molar mass of the unimer becomes larger. Thus a crosslinked c-PS-star sample of high R_g has less branches and is less polydisperse than a c-PCyan sample of the same R_g.

We think the observed behavior can be explained by these two arguments. Due to the large polydispersity of the c-PCyan and c-PEst systems the q regime is not reached where $\Gamma(q) \sim q^3$ is fulfilled and the Γ^* value still decreases in a qR_h regime where monodisperse, linear systems have already reached their asymptotic behavior. In this regime, the internal motions of the

large clusters are superimposed upon the translational motion of the smaller clusters. Information on the internal mobility can still be obtained by examining the absolute values of $\Gamma^*(q)$. They drop below the asymptotically constant value of linear chains at θ conditions. Note that the fractal dimension of clusters at good solvent conditions is similar to that of linear chains at θ conditions ($d_{fr} = 2$). The internal motions are here determined *by sections of the clusters which include branching points* and still guarantee self-similarity to the complete branched clusters ($d_{fr} \cong 2.2$). In contrast, for the internal motions probed in the c-PS-star system with its large basic unit and lower polydispersity, a plateau value is reached which is nearly that of linear chains in a good solvent ($d_{fr} = 1.67$), indicating that here *linear sections of the clusters* dominate the internal dynamics. The q regime where translational diffusion from small clusters and internal motions from large clusters contribute is apparently hidden in the region of the fast decay of $\Gamma^*(q)$ at low qR_h.

Martin et al.[5c] and Delsanti et al.[5d] studied prior to us the asymptotic regime with branched systems, but unfortunately did not publish the absolute $\Gamma^*(q)$ values. However, the mentioned findings for the power law, $\Gamma(q) \sim q^{2.8}$ for the silica gel system and $\Gamma(q) \sim q^3$ for polystyrene/divinylbenzene system, indicate that similar arguments as applied to our systems can be used to explain the differing exponents. Silica gel is a system with a small basic unit and resembles the c-PCyan system, whereas the styrene/divinylbezene copolymer, consisting of connected long chains with only a few branching points, corresponds more to the c-PS-star polymers.

These considerations suggest that we are dealing with two limiting cases: In the first case, the branching density is high, the distance between two branching points is small, and the width of the size distribution is very broad. In this case, we will observe a superposition of internal modes of the large clusters and translational motions of the smaller clusters in the ensemble. The internal modes are determined by branched sections of the clusters. In the second case the distance between two branching points is large, the branching density is low, and the polydispersity is moderate. Then the behavior of linear sections will dominate, and the superposition regime will be shifted into a q regime where translational diffusion dominates anyway.

The discussion of this section may be closed with two questions yet to be answered.

(1) Will $\Gamma^*(q)$ for the highly branched case (c-PCyan, c-PEst-chain) eventually reach a plateau with a value $\Gamma^*(\infty)$ characteristic of internal motions of branched sections, or will it increase further to reach the plateau value obtained for linear systems at similar solvent conditions?

(2) Is the $q^{2.8}$ dependence found for the higher branched systems really due to polydispersity or is it possibly the result of a hindered internal mobility in branched systems? The q^3 dependence of the first cumulant predicted for linear systems may not necessarily hold for densely branched systems in which the constraint exerted by branching points may have a nonnegligible influence.

Dynamic Light Scattering: The Shape Function. The first cumulant in dynamic LS represents only the initial part of the time correlation function. The whole TCF is sufficiently well-defined by $\Gamma(q)$ when only translational diffusion is observed. Then we have[19]

$$g_1(q,t) = \exp(-\Gamma(q)t) \tag{12}$$

with

$$\Gamma(q) = Dq^2$$

For the limit of very long chains, where only internal motions are probed ($qR_g \gg 1$), it was shown by de Gennes and Dubois-Violette[16] that the TCF can be scaled as a function of a dimensionless time

$$g_1(q,t) = \exp\{f[t/t^*]\} \tag{13}$$

where t^* is a characteristic time and $f[t/t^*]$ the so-called shape function. This expression has for very long delay times the asymptotic form of a stretched exponential

$$g_1(q,t) \rightarrow b \exp\left[-a\left(\frac{t}{t^*}\right)^{\beta}\right] \tag{14}$$

with exponents of $\beta = {}^2/_3$ for nondrained chains (Zimm limit) and $\beta = {}^1/_2$ for free draining (Rouse limit). Later in 1980 Akcasu et al.[15] took up the problem once again, derived equations for chains of finite chain length, and developed a method for the interpretation of dynamic light scattering experiments in terms of the first cumulant over the full range of q, including the transition range from $qR_g \ll 1$ to $qR_g \gg 1$. They observed that for $qR_g > 2$ the correlation functions can be scaled when $\Gamma(q)t$ is chosen as a dimensionless time scale, $\Gamma(q)$ being here the first cumulant, simply determined as the initial slope of the correlation function.

No predictions have been made so far for branched clusters, but it is of interest whether such shape functions also exist for branched macromolecules. This was tested experimentally by plotting the correlation functions obtained at different q vs the dimensionless time scale $\Gamma(q)t$.

We first checked in the low qR_g regime how the broad distribution in the randomly branched systems influences the TCF. Figure 6 shows the correlation functions from a branched and a linear low molar mass polyester (linear, $M_w = 103\,000$; branched, $M_w = 172\,000$). The linear polyester had a rather narrow size distribution ($M_w/M_n = 1.3$), the branched one a rather broad ($M_w/M_n = 6-7$). For both samples the regime of small qR_g is probed where translational motions dominate ($qR_g \ll 1$, no angular dependence in static LS). The effect of polydispersity is clearly seen. The correlation functions

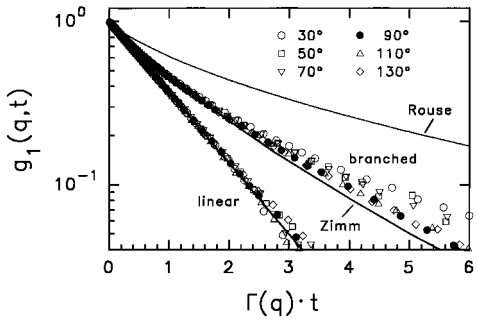

Figure 6. Plot of $g_1(q,t)$ vs the dimensionless time scale $\Gamma(q)t$. Correlation functions were obtained at various angles for a branched, *polydisperse* c-PEst-chain sample and a corresponding linear, *monodisperse* polyester sample of low molecular weight ($qR_g \ll 1$). For comparison, the shape functions predicted[15c] for linear systems in the Zimm and Rouse limits are also plotted.

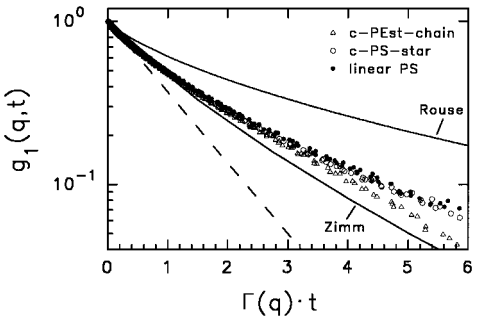

Figure 7. Plot of $g_1(q,t)$ vs the dimensionless time scale $\Gamma(q)t$. Correlation functions obtained at $qR_g > 3$ for the branched systems c-PEst-chain and c-PS-star and for a polystyrene chain sample in comparison to the predicted[15c] shape functions for linear chains in the Zimm and Rouse limits.

from the randomly branched, *polydisperse* polyester do not form a universal master curve and exhibit a stretched exponential behavior, whereas the linear, *narrowly distributed* polyester exhibits the expected almost single exponential behavior. In Figure 6 the shape functions predicted[15c] for internal motions of the linear chains in the Zimm and Rouse limits are plotted for comparison. The molecular weight distribution of the randomly branched system leads obviously to a superposition of exponential functions resulting in a stretch exponential behavior which is similar to that predicted for internal motions with hydrodynamic interaction (Zimm). This makes clear that it will be difficult to discern the influence of polydispersity from an effect of internal motions.

However, when samples are investigated in the regime from $qR_g < 1$ to $qR_g > 1$ one observes by fitting the TCFs with stretched exponential functions a change of the stretched exponent from $qR_g < 2$ ($\beta = 0.85-0.9$) to $qR_g > 3$ ($\beta < 0.85$). The change is small but consistently found for different c-PEst-chain samples. Finally, for $qR_g > 3$ *universal* behavior is found for the TCFs at various q of a given system. In Figure 7 the angular independent curves found for various samples of the c-PEst-chain and the c-PS-star systems are shown. In addition, the curve from a linear polystyrene chain in THF is shown. The two polystyrene systems, the linear and the branched one give the same shape function, and the long time tail can be fitted by a stretched exponential with $\beta = 0.64 \pm 0.04$ in good agreement with the predicted exponent for Zimm dynamics ($\beta = {}^2/_3$). For the c-PEst-chain system a slightly different curve is found. This may be not significant, since the scaling with respect to the first cumulant is involved with large errors, but the long time tail is here definitely not described by $\beta = {}^2/_3$ but by $\beta = 0.82 \pm 0.02$. Again the deviating behavior may be interpreted by the argument that for the wide mesh c-PS-star system the internal motions of linear sections are probed, whereas for the higher branched c-PEst-chain system branched sections of the clusters determine the internal motions. The findings reported in the literature for the already mentioned systems are in fair agreement with this interpretation. Martin et al.[5c] found no significant stretched exponential behavior for the highly branched silica gels, while Delsanti et al.[5d] could fit their data for crosslinked long-chain PS/DVB system with an exponent of $\beta = 0.67 \pm 0.05$.

In spite of a certain skepticism, concerning the possibility of a differentiation between the TCFs which are dominated by translational motions, but exhibit a stretched exponential behavior due to polydispersity and the TCFs which are mainly determined by internal motions, we can state that the dynamic scattering behavior of the branched systems is better described by Zimm relaxations with hydrodynamic interactions than by the Rouse spectrum with no hydrodynamic interactions. The q dependence of the first cumulant ($\Gamma \sim q^{2.8}$ and $\Gamma \sim q^3$) is close or equal to that expected in the Zimm limit, and the angular independent shape functions at $qR_g > 3$ exhibit approximately the predicted[15c] form for Zimm dynamics.

Conclusions

The present experiments with three randomly branched systems revealed that the effect of branching has an influence on the internal motions when the branching density is high. From an analysis of the asymptotic q dependence of the first cumulant alone it remains unclear whether the motions of the branching units influence the behavior or whether simply the very broad size distribution causes the observed effects. However, the analysis of the *absolute* values of the reduced cumulant $\Gamma^*(q)$ demonstrates that for the highly branched systems internal motions are indeed resulting from branched sections of the clusters, whereas for the less branched system internal motions of linear sections dominate. On the other hand, the variance in branching density was found to have no influence on the static particle scattering function.

Acknowledgment. This work was kindly supported by the Deutsche Forschungsgemeinschaft within the scheme of the SFB 60.

References and Notes

(1) (a) Flory, P. J. *J. Am. Chem. Soc.* **1941**, *63*, 3083, 3091, 3096. (b) Flory, P. J. *J. Phys. Chem.* **1942**, *46*, 132. (c) Stockmayer, W. H. *J. Chem. Phys.* **1943**, *11*, 45. (d) Stockmayer, W. H. *J. Chem. Phys.* **1944**, *12*, 125.

(2) (a) Stauffer, D.; Cognilio, A.; Adam, M. *Adv. Polym. Sci.* **1982**, *44*, 103. (b) Stauffer, D. *Introduction to Percolation Theory*; Taylor & Francis: Philadelphia, PA, 1985.

(3) for example: (a) Schmidt, M.; Burchard, W. *Macromolecules* **1981**, *14*, 370. (b) Schosseler F., Leibler, L. *J. Phys. Lett. (Fr.)* **1984**, *45*, L501. (c) Bouchaud, E.; Delsanti, M.; Adam, M.; Daoud, M.; Durand, D. *J. Phys. (Fr.)* **1986**, *47*, 1273. (d) Adam, M.; Delsanti, M.; Munch, J. P.; Durand, D. *J. Phys. (Fr.)* **1987**, *48*, 1809. (e) Martin, J. E.; Wilcoxon, J.; Adolf, D. *Phys. Rev. A* **1987**, *36*, 1803. (f) Patton, E. V.; Wesson, J. A.; Rubinstein, M.; Wilson, J. C.; Oppenheimer, L. E. *Macromolecules* **1989**, *22*, 1946. (g) Schosseler, F.; Daoud, M.; Leibler, L. *J. Phys. (Fr.)* **1990**, *51*, 2373.

(4) (a) Adam, M.; Delsanti, M. *Macromolecules* **1977**, *10*, 1229. (b) Han, C. C.; Akcasu, A. Z. *Macromolecules* **1981**, *14*, 1080. (c) Tsunashima, Y.; Nemoto, N.; Kurata, M. *Macromolecules* **1983**, *16*, 1184. (d) Nemoto, N.; Makita, Y.; Tsunashima, Y.; Kurata, M. *Macromolecules* **1984**, *17*, 425. (e) Wiltzius, P.; Cannell, D. S. *Phys. Rev. Lett.* **1986**, *56(1)*, 61. (f) Tsunashima, Y.; Hirata, M.; Nemoto, N.; Kurata, M. *Macromolecules* **1987**, *20*, 1992. (g) Tsunashima, Y.; Hirata, M.; Nemoto, N.; Kajiwara, K.; Kurata, M. *Macromolecules* **1987**, *20*, 2862. (h) Bhatt, M.; Jamieson, A. M. *Macromolecules* **1988**, *21*, 3015. (i) Bhatt, M.; Jamieson A. M.; Petschek R. G. *Macromolecules* **1989**, *22*, 1374.

(5) (a) Daoud, M. *J. Phys. (Fr.)* **1990**, *51*, 2843. (b) Benmouna, M.; Borsali, R.; Khaldi, S. *J. Polym. Sci., B: Polym. Phys.* **1995**, *33*, 1281. (c) Martin, J. E.; Wilcoxon, J.; Odinek, J. *Phys. Rev. A* **1991**, *43*, 858. (d) Delsanti, M.; Munch, J. P. *J. Phys. II (Fr.)* **1994**, *4*, 265.

(6) Bauer, M.; Bauer, J. In *The Chemistry and Technology of Cyanate Ester Resins*; Hamerton, I., Ed.; Chapman & Hall: Glasgow, Scotland, 1994.

(7) Matejka, L.; Lövy, J.; Pokorny, S.; Bouchal, K.; Dusek, K. *J. Polym. Sci., Chem. Ed.* **1983**, *21*, 2873.

(8) (a) Trappe, V.; Burchard, W.; Steinmann, B. *Macromolecules*

1991, *24*, 4738. (b) Trappe, V.; Burchard, W.; Steinmann, B. *Makromol. Chem., Macromol. Symp.* **1991**, *45*, 63.
(9) Bantle, S.; Schmidt, M.; Burchard, W. *Macromolecules* **1982**, *15*,1604.
(10) Trappe, V.; Richtering, W.; Burchard, W. *J. Phys. II (Fr.)* **1992**, *2*, 1453.
(11) Daoud, M.; Martin, J. E. in *The Fractal Approach to Heterogeneous Chemistry*; Avnir, D., Ed.; Wiley & Sons: New York, 1989.
(12) Bauer, J.; Dingenouts, N.; Ballauff, M. *Acta Polym.* **1994**, *45*, 430.
(13) Kallala, M.; Sanchez, C.; Cabane, B. *Phys. Rev. E* **1993**, *48*, 3692.
(14) Freltoft, T., Kjems, J. K.; Sinha, S. K. *Phys. Rev. B* **1986**, *33*, 269.
(15) (a) Benmouna, M.; Akcasu, A. Z. *Macromolecules* **1978**, *11*, 1187. (b) Benmouna, M.; Akcasu, A. Z. *Macromolecules* **1980**, *13*, 409. (c) Akcasu, A. Z.; Benmouna, M.; Han, C. C. *Polymer* **1980**, *21*, 866.
(16) (a) de Gennes, P. G. *Physics* **1967**, *3*, 37. (b) Dubois-Violette, E.; de Gennes, P. G. *Physics* **1967**, *3*, 181.
(17) Zimm, B. H. *J. Chem. Phys.* **1956**, *24*, 269.
(18) Rouse, P. E. *J. Chem. Phys.* **1953**, *21*, 1272.
(19) Berne, B. J.; Pecora, R. *Dynamic Light Scattering*; Wiley & Sons: New York, 1976.

MA961728W